

Article

Design and Preliminary Evaluation of a Precision Cylindrical Air-Assisted Drill Sowing Device for Rapeseed, Wheat, and Rice

Alfarog H. Albasheer ^{1,2}, Qingxi Liao ^{1,3,*}, Lei Wang ⁴, Anas Dafaallah Abdallah ⁵ and Jianxin Lin ¹

- ¹ College of Engineering, Huazhong Agricultural University, Wuhan 430070, China; forga209@webmail.hzau.edu.cn (A.H.A.); linjianxin2021@webmail.hzau.edu.cn (J.L.)
- ² Department of Agricultural Engineering, Faculty of Agriculture and Natural Resources, University of Bakht Al-Ruda, Ed Dueim P.O. Box 1311, Sudan
- ³ Key Laboratory of Agricultural Equipment in Mid-lower Yangtze River, Ministry of Agriculture and Rural Affairs, Wuhan 430070, China
- ⁴ College of Engineering, Nanjing Agricultural University, Nanjing 210031, China; leiwang@njau.edu.cn
- ⁵ Department of Agricultural Engineering, Faculty of Agricultural Science, University of Gezira, Wad Medani P.O. Box 20, Sudan; anas@webmail.hzau.edu.cn
- * Correspondence: liaoqx@mail.hzau.edu.cn

Abstract: To address challenges in seed feeding stability and seeding uniformity in agricultural practices, this study aimed to introduce a cylindrical air-assisted drill sowing device (CADSD) designed for rapeseed, wheat, and rice (RWR). The device features a prototype hill-feeding mechanism that addresses problems related to seed feeding, airflow disruptions, and seed-wall collisions. Comprehensive bench tests, Discrete Element Method (DEM) simulations, and preliminary field experiments were conducted to evaluate the seed-feeding stability characteristics and optimize the structural parameters of the air-assisted drill sowing system, enhancing seeding uniformity and operational efficiency. The optimal operating speed range is between 4 and 5 km/h. When the seed feeding speed is 30 to 38 r/min, the coefficient of variation of the seed supply rate stability is less than 0.55%, and the relative error between the theoretical and the experimental actual values of the RWR supply rate regression model is less than 2%, further supporting the effectiveness of the device. A preliminary field test revealed a seeding uniformity coefficient of variation (CV) of 3.44% and an emergence rate of 88%, closely aligning with the desired metrics. The CADSD effectively sows multiple crop types with improved precision and uniformity, handling diverse seed types and sizes without requiring equipment modifications, highlighting its innovative impact on agricultural technology in the precise seeding of RWR.

Keywords: precision seeding; air-assisted drill; hill-feeding mechanism; rapeseed; wheat; rice; seed supply device



Citation: Albasheer, A.H.; Liao, Q.; Wang, L.; Abdallah, A.D.; Lin, J. Design and Preliminary Evaluation of a Precision Cylindrical Air-Assisted Drill Sowing Device for Rapeseed, Wheat, and Rice. *Agriculture* **2024**, *14*, 2355. <https://doi.org/10.3390/agriculture14122355>

Academic Editor: Jin He

Received: 12 November 2024

Revised: 30 November 2024

Accepted: 16 December 2024

Published: 21 December 2024



Copyright: © 2024 by the authors. Licensee MDPI, Basel, Switzerland. This article is an open access article distributed under the terms and conditions of the Creative Commons Attribution (CC BY) license (<https://creativecommons.org/licenses/by/4.0/>).

1. Introduction

RWR are essential oil crops and food supplies in the mid-lower Yangtze area of China and worldwide [1,2]. Rapeseed and wheat are planted in the autumn after the rice harvest. The planting methodologies for these crops are very similar [3,4]. Seeding is a crucial task in cereal cultivation, given that the appropriate technology and precise adjustment of seeding rates based on particular soil and climatic conditions significantly impact forthcoming yields [5,6]. The uniformity of seeding serves as a vital indicator for assessing the sowing efficiency of a planter [7,8]. It is significant in achieving the correct population distribution and maximizing yield for RWR [9]. The level of operation of the seed metering is determined by its precision. Recognizing the importance of precise sowing can minimize seed consumption during field operations, lower seed expenses, and enhance the benefits of planting [10,11].

The metering device is the drill seeder's most essential component [12]. Metering devices are classified into two types: single-row and centralized. Due to the advantages of multi-row seeding, flexible width, and fast seed loading and unloading, the CADSD has become a standard metering device for sowing cereals in Western countries [13,14]. Centralized pneumatic planters are capable of handling a wide range of seeds at high sowing speeds and across large widths. This versatility significantly enhances seeding efficiency, making them suitable for various seeding applications [15]. The CADSD is extensively used to seed RWR and other crops. It is fundamental in producing large-scale no-tillage seeders by multiple companies, including John Deere in the United States, Amazon in Germany, and Maschio in Italy [9]. Drilling is a recommended sowing method because it ensures a uniform seed population per unit area; this method promotes high germination rates and even stands [16,17].

Global scientific investigations have been undertaken to enhance the efficacy of seed metering equipment. Previous studies have focused explicitly on the design and performance of the air-assisted centralized seed-metering mechanism. Yatskul et al. [18] studied the uniformity of seed distribution through the outlet dividers employing the Kuhn seeder; the researchers uncovered the necessity for an even division of air-seed flow by the distribution head before transportation to the soil. Kumar and Durairaj [19] analyzed the distribution uniformity among various distribution head structures. Mudarisov et al. [20] demonstrated the superior effectiveness of a streamlined flow structure in enhancing distribution uniformity. Zhang et al. [21] conducted extensive research on a grain seeder, wherein a centralized air-assisted seeding system was designed, and the structural parameters of the distribution system were meticulously optimized for wheat.

Designing a sowing device for a universal combine seeder that can handle a variety of crops is a complex task that involves optimizing for multiple factors such as seed type, sowing pattern, and operational efficiency. Developing a combined direct seeder can significantly improve equipment utilization and reduce production costs [15]. Due to the significant differences in material characteristics and seeding rates per unit area, separate seeders are currently used for sowing RWR [22]. However, to enhance the versatility of seeders, scholars have recently conducted research on multi-crop sowing technology and multi-crop sowing devices. Akhalaya et al. [23] designed a seeder that can feature combining individual dots or patterns without changing the components. The ability to adapt is critical when using various planting procedures for different crops.

Furthermore, a study by Tarasekomet et al. [24] focused on improving the design and technology of mechanical sowing equipment in order to address the difficulty of efficiently planting small seed crops by upgrading the design and technology used in mechanical planting tools. Baoshan et al. [25] designed and improved a metering device with inclined parabolic holes and stirring structures to enhance seed-filling performance for small seed crops: rapeseed, sesame, and pakchoi. Li Xiaoran et al. [26] studied a type hole wheel with a high-speed air-assisted centralized metering device for rice, wheat, and rapeseed; the research demonstrated how structural adjustments in the model-hole design improved the precision in seed placement and reduced variation in seed feeding quantity. Previous studies have shown that sowing machines designed for planting multiple crops with varying seed sizes require the replacement of certain components in the metering device. Therefore, our study aimed to design a CADSD that can eliminate the need for these adjustments. The mechanism includes two specialized hole wheels designed for sowing different seed sizes, including RWR. This reduces operational complexity and costs, making it a versatile solution for precision agriculture. Additionally, the performance, discharge stability, and row discharge consistency were investigated using DEM software, bench tests, and preliminary field tests to modify and optimize the device operating and design parameters for advanced performance investigation.

2. Materials and Methods

2.1. Basic Physical Properties of Rapeseed, Wheat, and Rice

The essential properties of RWR seeds' physical and engineering properties play a crucial role in advancing agricultural technology. Precise determination of parameters, such as size, dimensions, capacity, mass, specific gravity, surface area, and other mechanical characteristics, is crucial for effectively guiding the design process, whether evaluating the material in large quantities or as separate entities [27]. Tables 1 and 2 show the physical and mechanical properties of RWR.

Table 1. Physical properties of RWR.

Crop	Length (mm)	Width (mm)	Thickness (mm)	Sphericity %	1000 Seed Mass, (g)	Angle of Repose (°)
Wheat (Lei Xiaoping 9023)	6.30	3.09	2.75	45.63	44.87	28.22
Rice (Quanyou 737)	10.9	2.9	2.2	36.24	24.05	28.81
Rapeseed (Huayouze 62)	2.26	2.07	2.01	95.50	3.83	22.72

Note: Sphericity is defined as the ratio of the diameter of the largest inscribed circle to the diameter of the largest circumscribed circle of the seed.

Table 2. Mechanical properties of RWR.

Parameter	Rapeseed	Wheat	Rice	Aluminum Alloy	Engineering Plastic ABS
Three axes diminution mm ³	2 × 2 × 2	6 × 3 × 3	10.2 × 3 × 2		
Density kg/m ³	1060	1350	1125	2700	1060
Poisson's ratio	0.25	0.42	0.30	0.30	0.394
Shear modules/pa	1.1 × 10 ⁷	5.1 × 10 ⁷	1.01 × 10 ⁸	2.7 × 10 ¹⁰	8.96 × 10 ⁸
Collision recovery coefficient	Seed-seed	0.60	0.42	0.50	
	SAA	0.60	0.50	0.45	
	Seed-ABS	0.75	0.60	0.001	
Static friction coefficient	Seed-seed	0.50	0.35	0.50	
	SAA	0.30	0.40	0.57	
	Seed-ABS	0.30	0.40	1.0	
Dynamic friction coefficient	Seed-seed	0.01	0.05	0.01	
	SAA	0.01	0.05	0.01	
	Seed-ABS	0.01	0.05	1.03	

Note: SAA seed–aluminum alloy, ABS Acrylonitrile butadiene styrene copolymer.

2.2. The Overall Structure and Working Principle

The CADSD comprises key components, including a high-pressure blower, seed box, centralized seed-feeding device, Venturi feeding device, seed conveying pipe, booster pipe, distribution head, and double disc ditchers, as seen in Figure 1. During operation, the high-pressure blower supplies consistent air pressure, enabling seeds from the seed box to be transported via the centralized seed-feeding device into a Venturi tube. With air pressure, the seeds are scattered and slowed down by the booster pipe before reaching the distributor. The 8-row distributor ensures that the seeds are uniformly distributed. The seeds are then planted into the soil using the seed delivery pipe and the double disc ditcher.

The crucial part of the CADSD is the prototype centralized seed-feeding device, consisting of a seed-feeding shell, seed-filling chamber, seed-filling regulating plate, and seed-feeding mechanism (Figure 2a). The seed-feeding mechanism consists of two specialized hole wheels—one for rapeseed seeds and another for wheat and rice seeds—along with components such as a blank wheel, a diaphragm, a transmission shaft, and a seed

barrier, which divides the seed shell into two portions (Figure 2b). During sowing, wheat or rice seeds in the seed box are directed into the seed-filling chamber through the force of gravity. The seeds are subsequently transferred into the holes of the seed-feeding mechanism's particular hole wheel within the seed-filling chamber. This transfer occurs due to the lateral pressure carried on by the seed population and the disturbance caused by the hole wheel's rotation. The seeds are filled precisely through the seed-filling gap produced by the seed-filling adjustment board and the seed-feeding mechanism. This is achieved by placing the seeds in the appropriate type of hole. By rotating the hole wheel, wheat or rice seeds are directed into the Venturi tube via gravity and centrifugal force. The process is similar for rapeseed, ensuring an efficient and steady seed supply for all types.

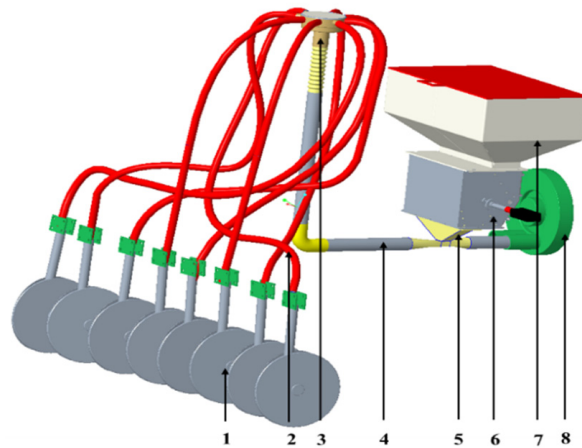
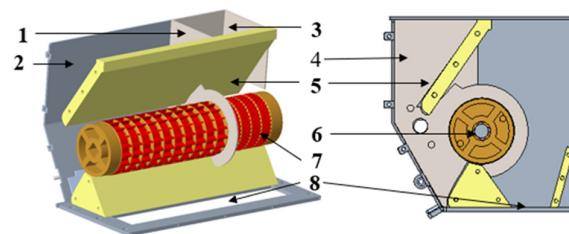
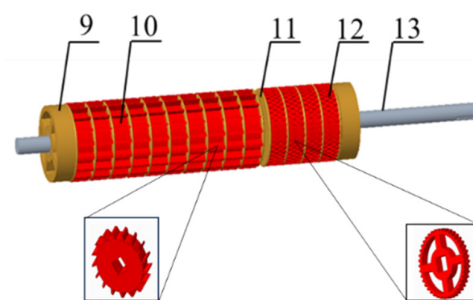


Figure 1. Schematic diagram of an air-assisted centralized metering system for RWR. 1. Double disc dishes. 2. Seed delivery pipe. 3. Distributor 4. Booster pipe. 5. Venturi tube 6. Centralize seed feeding device. 7. Seed box. 8. High-pressure blower.



(a)



(b)

Figure 2. Sketch of the centralized seed-feeding device; (a) RWR shell sections and barrier Structure of centralized seed-feeding device; (b) Seed feeding mechanism. 1. Shell section barrier; 2. Wheat and rice section; 3. Rapeseed section; 4. Seed shell; 5. Seed layer; 6. Seed feeding mechanism; 7. Prototype hole wheel; 8. Seed fall mouth; 9. Blank wheel; 10. Wheat and rice hole wheel; 11. Division plate; 12. Rapeseed hole wheel; 13. Transmission shaft.

2.3. Mechanical Analysis of the Working Process of the Seed Plant
 2.3.1. Mechanical Analysis of Seed Population in Filling Zone

The seed filling performance is crucial for the stability of seed supply, which can be improved by optimizing hole structure and increasing filling force. As seeds move in an arc shape within the filling area, the population in the forced movement area is considered the seed flow of the rectangular section (the surface spacing thickness between the contact surface and the cone hole wheel). The population microsegment in the filling area is the study object. Figure 3 shows the force analysis in the filling area. In this area, the lateral pressure (F_n) on the population affects seed flow, primarily causing lateral pressure (F_n). Due to effective supply, the seed flow easily fills the hole. The force analysis of the microsegment in the filling region establishes the force balance equation:

$$\begin{cases} F_N \cos\theta - F_n \sin\beta - F_f \sin\theta = G \cos\beta \\ F_n \cos\beta + F_f \cos\theta + F_N \sin\theta - G \sin\beta \geq F_c \\ F_f = \mu F_N \\ F_c = m\omega^2 r \end{cases} \quad (1)$$

where m is the mass of the population microsegment, kg, G is the gravity of population segments, N , F_f is the friction between microsegments and holes of the population, N , F_n is the lateral pressure of the population on the microsegments of the population, N , F_c is the inertial centrifugal force of the population microsegment, N , F_N is the type pore supports the population microsegment, N , ω is the angular speed of the cone hole wheel, rad/s, g is the gravity acceleration, m/s^2 , M is the friction coefficient between the cone hole wheel and seed, 0.3 for rape seed and 0.55 for wheat seed, β is the Angle between the y -axis and the horizontal plane ($^\circ$), θ is the type hole inclination, ($^\circ$), and r is the radius of the cone hole wheel, m.

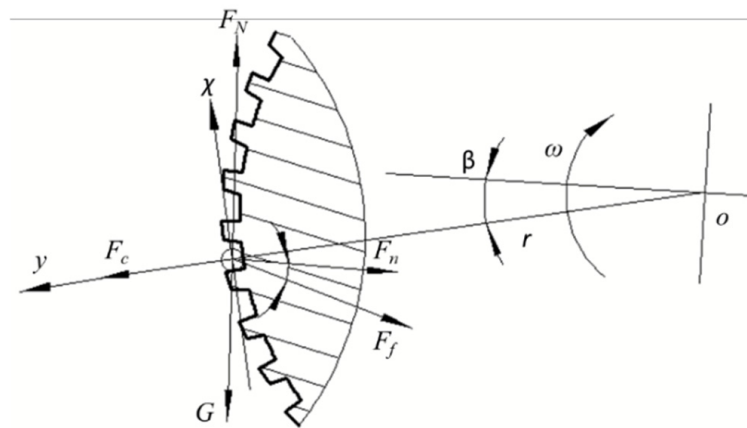


Figure 3. Mechanics analysis of seeds population in filling zone. ω is the angular velocity of the cone hole wheel; r is the radius of the cone hole wheel; β is the seed’s initial filling position; F_f is the friction between microsegments and holes of the population; F_n is the lateral pressure of the population on the microsegments of the population; F_N is the type pore supports the population microsegment; x is x -axis; G is the gravity of population segments; F_c is the inertial centrifugal force of the population microsegment; y is y -axis.

From Formula (1):

$$\beta \geq \arccos\left(\frac{\omega^2 r}{g\sqrt{1+K^2}}\right) - \arctan\left(\frac{1}{K}\right) \quad (2)$$

$$K = \frac{\mu \cos\theta + \sin\theta}{\cos\theta - \mu \sin\theta} \quad (3)$$

Equation (2) demonstrates a relationship between the seed initial filling position β and the seed material characteristic μ , the hole structure parameter θ , and the cone wheel angular velocity ω . When the angular velocity ω is constant, the initial filling position β positively correlates with the inclination θ ; at the same initial filling position β , the inclination θ increases with the angular velocity ω . The initial filling position β must be less than the unloading angle γ , specifically $\beta < 30^\circ$, with a rotation speed range of 30–40 r/min. The friction coefficient between rape, wheat, and rice seeds and the cone wheel determines the range of the hole inclination angle θ , which is found to be 13.75–21.20°.

2.3.2. Mechanical Analysis of Seed Population in Feeding Zone

The perforated hole containing seeds rotates about the axis within the seeding region, transitioning to the seed-feeding area. Upon entering the seed-feeding area, the angle between the seed center and the axis relative to the horizontal plane is denoted as ϵ . The force analysis of the seed during this process is illustrated in Figure 4. In conditions critical to seed supply, the equilibrium equation [15] is expressed in Equation (4).

$$\begin{cases} G \cos \epsilon - F_{N1} \cos \theta - F_f \sin \theta = 0 \\ F_c - G \sin \epsilon + F_{N1} \sin \theta - F_f \cos \theta = 0 \\ F_f = \mu F_{N1} \\ F_c = m \omega^2 r \end{cases} \quad (4)$$

where F_{N1} is the type hole for the seed support force, N, and ϵ is the angle between the axis and the horizontal plane, (°).

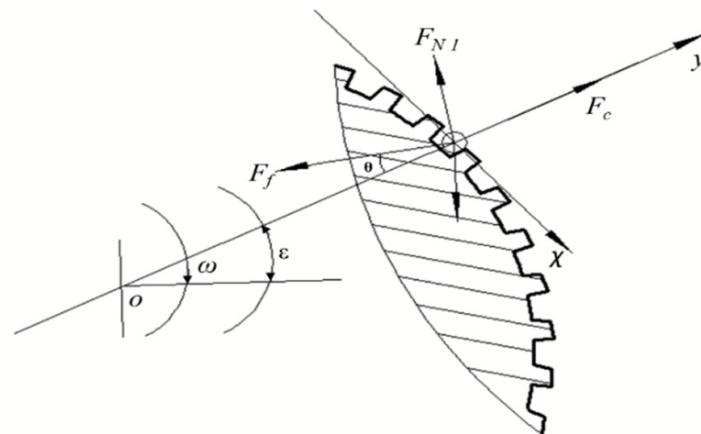


Figure 4. Mechanics analysis of seeds in the feeding zone. ω is the angular velocity; ϵ is the angle between the axis and the horizontal plane; F_f is the friction between microsegments and holes of the population; θ is the hole inclination angle; F_{N1} is the type pore supports the population microsegment; x is the x -axis; F_c is the inertial centrifugal force of the population microsegment; y is the y -axis.

From Equation (4):

$$\omega = \sqrt{\frac{\sin(\epsilon - \theta) + \mu \cos(\epsilon - \theta)}{r(\cos \theta + \mu \sin \theta)}} \quad (5)$$

According to Equation (5), ϵ increases notably with the rise in θ at a consistent speed. This indicates that the determined hole inclination angle θ advances the position of the seed supply, extending the seed supply duration and reducing blockage occurrence in hole types. The elevated angle of the cone-cylindrical hole's centerline to the wall, which is greater than that of the cylindrical hole, results in a substantial increase in feeding time. Additionally, the centrifugal force on seeds, which escalates with higher speeds, contributes to an increase in ϵ . Due to the lower friction coefficient between rapeseed seeds and the cone-hole wheel

compared to wheat and rice seeds, the initial seed supply angle increases significantly, indicating superior mobility of rapeseed seeds and enhanced seed supply performance.

2.4. Type Hole Shape

Due to the significant difference in seed material characteristics and seed volume per unit area, the hole size of the seed plant is based on rice seeds in the wheat and rice wheel drum. Rapeseed seeds have high sphericity and fluidity, making it easy to fill the hole; wheat and rice seeds are ellipsoid. According to their physical and mechanical characteristics, they may be positioned on the side, lying flat, or erect [28]. Theoretical studies show that the probability of the seed capsule entry hole state is proportional to the cross-sectional area of the state, namely:

$$\frac{P_F}{P_L} = \frac{S_F}{S_L} \frac{P_F}{P_E} = \frac{S_F}{S_E} \frac{P_L}{P_E} = \frac{S_L}{S_E} \quad (6)$$

where P_F is the seed lying flat posture probability, %, P_L is the probability of seed lateral posture, %, P_E is the seed standing posture probability, %, S_F is the seed posture cross-sectional area, mm^2 , S_L is the cross-sectional area of the seed side, mm^2 , and S_E is the sectional area, mm^2 .

The probability of the seed capsule entry hole pose is an incompatible event, and the sum is equal to 1, namely:

$$P_F + P_L + P_E = 1 \quad (7)$$

The shape of wheat and rice seeds is ellipsoid, and the cross-sectional area of different capsule hole poses is as follows:

$$S_F = \frac{\pi}{4}lw, S_L = \frac{\pi}{4}lt, S_E = \frac{\pi}{4}wt \quad (8)$$

where l is the seed length, mm, w is the seed width, mm, and t is the seed thickness, mm.

In the filling area, seeds rely on lateral pressure and the cone wheel's disturbance to fill the hole. Optimizing the hole structure under lateral pressure improves seed-filling performance. The structure is designed to facilitate seed filling in flat and lateral holes; the hole inclination angle is θ , the cross-section is cylindrical, and the cone angle δ is 14° . The combination of the seed supply device and experimental study shows that the hole shape is suitable for rice, wheat, and rape. The oblique teeth formed between type holes enhance the perturbation of the population, and the type hole cross-section is shown in Figure 5.

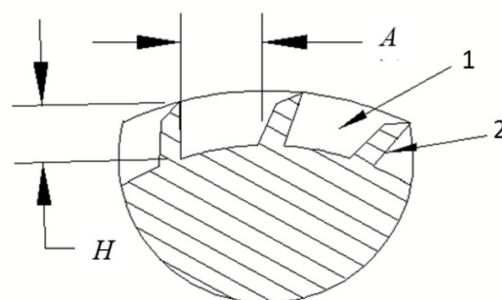


Figure 5. Sectional structure of model-hole. 1. Type hole; 2. Skew gear tooth; (A) the type hole width, mm; (H) the type hole depth, mm.

2.5. Type Hole Size

Based on RWR physical and mechanical characteristics, they may be positioned on the side, lying flat, or erect [28]. To prevent wheat and rice seeds from clogging the holes and to ensure filling, a single type of hole should accommodate 1–2 rapeseed seeds and

1–6 wheat and rice seeds. According to the empirical formula [29], the hole length (L), hole width (A), and hole depth (H) are defined as follows:

$$L = L_{max} + K_L \quad (9)$$

$$A = K_A W_{max} \quad (10)$$

$$H = K_H W_{max} \quad (11)$$

where L is the shaped hole length, mm, L_{max} is the maximum length of the seed, mm, K_L is length increment, mm (1.0~1.5), A is type hole width, mm, K_A is the width adjustment coefficient (1.1~1.3), H is the type hole depth, mm, K_H is the depth adjustment coefficient, (0.9~1.1), and W_{max} is the maximum width of the seed, mm.

Table 1 displays the required dimensions for rice, wheat, and rapeseed. For rice, W_{max} and L_{max} should be 3.6 mm and 10.9 mm, respectively. As for rapeseed, the values are 2.07 mm and 2.26 mm. The hole size triaxial dimensions for rice seeds are L 16 mm, A 5.0 mm, and H 4.0 mm, while rapeseed are L 3.7 mm, A 2.5 mm, and H 2 mm.

2.6. DEM Establishment

The DEM facilitates interaction among agricultural machinery components [26]. We integrated a simplified multi-seed planter model into DEM Software's pre-processing module (Version 2020). We used the multi-spherical aggregation approach to examine the motion and filling process of RWR seeds. To depict the irregular shape of the seeds, we used seven soft sphere models with diameters of 2.5 mm and 3 mm based on the measured physical characteristics of various RWR seeds.

The seeder's model was generated in Pro/E 5.0 and loaded into DEM software, which was simplified into three components: the shell, seed feeding mechanism, and shell section barrier. The materials used were aluminum alloy for the shell and engineering plastic and ABS (Acrylonitrile-butadiene-styrene copolymer) for the seed-feeding mechanism and shell section barrier. The simulation settings, including the Hertz–Mindlin non-sliding contact model between the seed and seed feeding mechanism, were established as specified in Table 2. The seed mechanism simulation models for rice and wheat had 10 wheel holes, while the simulation model for rapeseed had only 4 wheel holes. These changes simplified the DEM processing module model, allowing efficient seed movement into filling rooms. Figure 6d shows the simulation models created for the seed supply metering device. Seed shapes were simulated with dimensions of rapeseed 2 mm × 2 mm × 2 mm, wheat 8 mm × 3 mm × 3 mm, and rice 10 mm × 3 mm × 2 mm, as shown in Figure 6a–c, with a standard deviation of 0.05 mm.

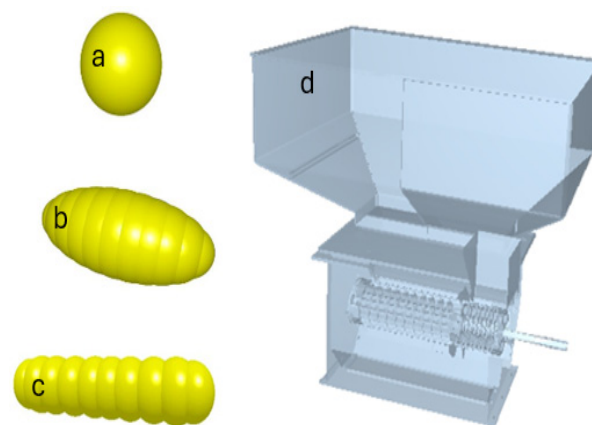


Figure 6. DEM simulation model. (a) Rapeseed seed; (b) Wheat seed; (c) Rice seed; (d) Seed supply metering device.

3. Experiments

3.1. Simulation Model Verification

The total simulation time was set to 8 s for rice and wheat and 6 s for the rapeseed pellet factory. A total of 5000, 3500, and 1000 grains for wheat, rice, and rapeseed, respectively, were used based on the sizes of the seeds and the seed shell sections. To simulate the actual situation, the particle factory seed generation time was set from 0 to 4 s, and the seeds were kept for 4 s; the hole wheel rotated starting from the 4th second. According to the stable charge limit speed found in the initial test, the hole wheel speed was set to 30 r/min and 38 r/min. After the simulation, the DEM post-processing module was used to observe the state of population movement in the seed supply stage. The change curve of the number of seeds supplied by the seed device under different arrangements of the extraction hole wheel was analyzed, the stability differences of seeds under various arrangement methods were compared, and the average seed quantity and coefficient of variation within the test time were statistically analyzed.

3.2. Bench Test Verification

The CADSD for RWR was subjected to a bench performance test at the seed arrangement performance laboratory of Huazhong Agricultural University to validate its actual working performance. The test was conducted using the test bench shown in Figure 7. The test materials included wheat, rice, and rapeseed. The moisture content of the test seeds was 8.69% for wheat, 10.78% for rice, and 7.18% for rapeseed; the impact of seed moisture on feeding performance was acknowledged, with variations potentially affecting seed flowability and uniformity. These moisture levels were controlled to ensure consistent seed behavior during testing. The other physical characteristic parameter values are specified in Table 1.

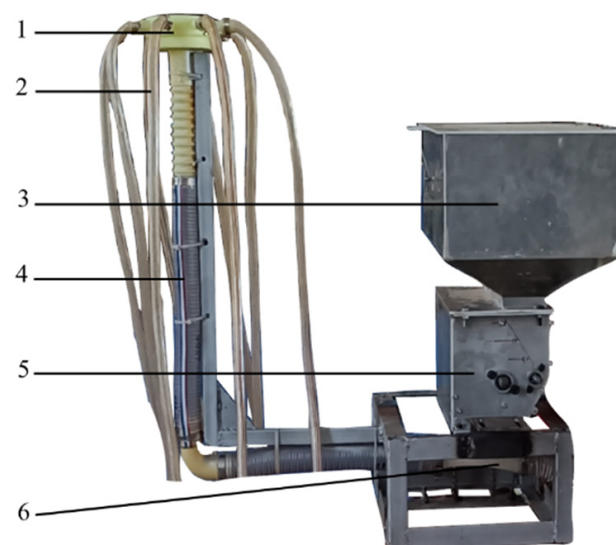


Figure 7. Seed metering performance test bench. 1. Distribution device; 2. Seed guide pipe; 3. Seed box; 4. Transmission pipeline; 5. RWR seed supply device; 6. Venturi tube.

The test conducted a single-factor test of seed supply speed according to the GB/T 25418-2022 Standard Test [30]. The purpose was to investigate the effect of the main parameters on seed supply for each crop, develop a regression model for the seed supply rates of RWR, and identify the best combination of parameter values. The factors considered in the experiment were the hole wheel speed and the air pressure of the fan. The evaluation

criteria for the test included the seed supply rate and the coefficient of stability of the seed supply rate [26,31].

$$\left\{ \begin{array}{l} m_v = \frac{\sum_{i=1}^j m_{vi}}{j} \\ C_V = \frac{\sqrt{\frac{1}{j-1} \sum_{i=1}^j (m_{vi} - m_v)^2}}{m_v} \times 100\% \\ P_z = \frac{m_p}{m_z} \times 100\% \end{array} \right. \quad (12)$$

where m_v is the average seed supply rate, g/min, m_{vi} is the seed supply rate of i , g/min, j is the test number ($j = 5$), C_V is the stability variation coefficient of the seed supply rate, %, P_z is the seed breakage rate, %, m_p is the damaged seed mass, g, and m_z is the total seed supply mass of each test, g.

To demonstrate the impact of the hole wheel speed of the seed drill on the seed feed rate, we conducted additional experiments. This study aims to establish the relationship between the rotation working speed of the hole wheel in the CADSD, the density of seeds sown, and the feeding rate. The experiment involved two independent factors: the density of the seeds (Y) and the hole wheel working speed (X), as shown in Table 3. Both factors were varied across three levels using rapeseed (density: 1060 kg/m³), rice (density: 1125 kg/m³), and wheat (density: 1350 kg/m³). The working speed levels were 3, 4, and 5 km/h. Measurements were conducted with five replications for each point of the experimental plan.

Table 3. Plan of the experiment: independent variables.

X, (km/h)	Y, (kg/m ³)
3	1060
3	1125
3	1350
4	1060
4	1125
4	1350
5	1060
5	1125
5	1350

Finally, to assess the accuracy of the CADSD, we conducted a regression validation test between the theoretical feed rate and actual test feed rate (g/m) at speeds of 4 km/h (30 rpm) and 5 km/h (38 r/min); an initial test demonstrated that the optimal operating speed for seed feeding lies between 4 and 5 km/h. During the verification test, the seed supply speed was adjusted to match the predicted values from the regression model. Five average measurements for each group were used, and the relative error between the test values and the theoretical values of the seed supply rate were compared.

3.3. Field Experiment Verification

The field experiment of rice sowing was conducted in the modern agricultural research and development base of Huazhong Agricultural University, Wuhan City, Hubei Province, in June 2024. The field seeding process is shown in Figure 8.

In the rice drought live broadcast experiment, Dongfeng LX-954 produced by Yancheng Shunyu Agricultural Machinery Co., Ltd., Yancheng City, China, was used as the traction power; the average operating speed was 4 km/h, the working width was 2 m, and the sowing was eight lines. The rice variety used in the experiments was *Quanyou 737*; the sowing volume was 37.5 kg/h, the sowing depth was 2 cm, and the sowing quantity was 60 g/min.



Figure 8. Field seeding test of rice.

After completing the large-scale field experiment and achieving uniformity among the seedlings, the checkerboard method selected five sampling points for the seed uniformity test. At each sampling point, the total number of rice seedlings within a 100 cm area was measured, and the average was calculated and then adjusted to determine the emergence rate per unit area of the field.

4. Results and Discussion

4.1. Analysis of DEM Simulation

The DEM post-processing module observed the population movement during the seed filling and falling stages, with movement states under different speed conditions for RWR shown in Figure 9. Figure 9b indicates that at a speed of 38 r/min, the filling stage is prominent. Some seeds do not fully enter the hole initially, but as the side wall of the hole rotates, the seeds are cast into the planting stage without getting stuck.

According to Figure 9, the DEM post-processing module extracted the quality of seeds discharged per second by the seed supply device. The variation coefficient of average seed supply and stability at 30 r/min and 38 r/min were analyzed. At a feeding speed of 30 r/min, the average seed supply of rice, wheat, and rape seeds within seconds 4 to 8 was 14.8 g/s, 33.06 g/s, and 4.46 g/s, respectively; the coefficient of variation of the feeding stability was 0.79%, 0.64%, and 0.23%, respectively. At a feeding speed of 38 r/min, the average seed supply of rice, wheat, and rapeseed seeds within seconds 4 to 8 was 25.31 g/s, 39.37 g/s, and 5.85 g/s, respectively. The coefficient of variation of the feeding stability was 1.6%, 1.8%, and 0.88%, respectively when the speed was 30 r/min, the stability coefficient was less than 0.8%. When the speed reached 38 r/min, the increase in the stability coefficient was apparent, with the coefficient of variation for RWR seeds exceeding 0.8%.

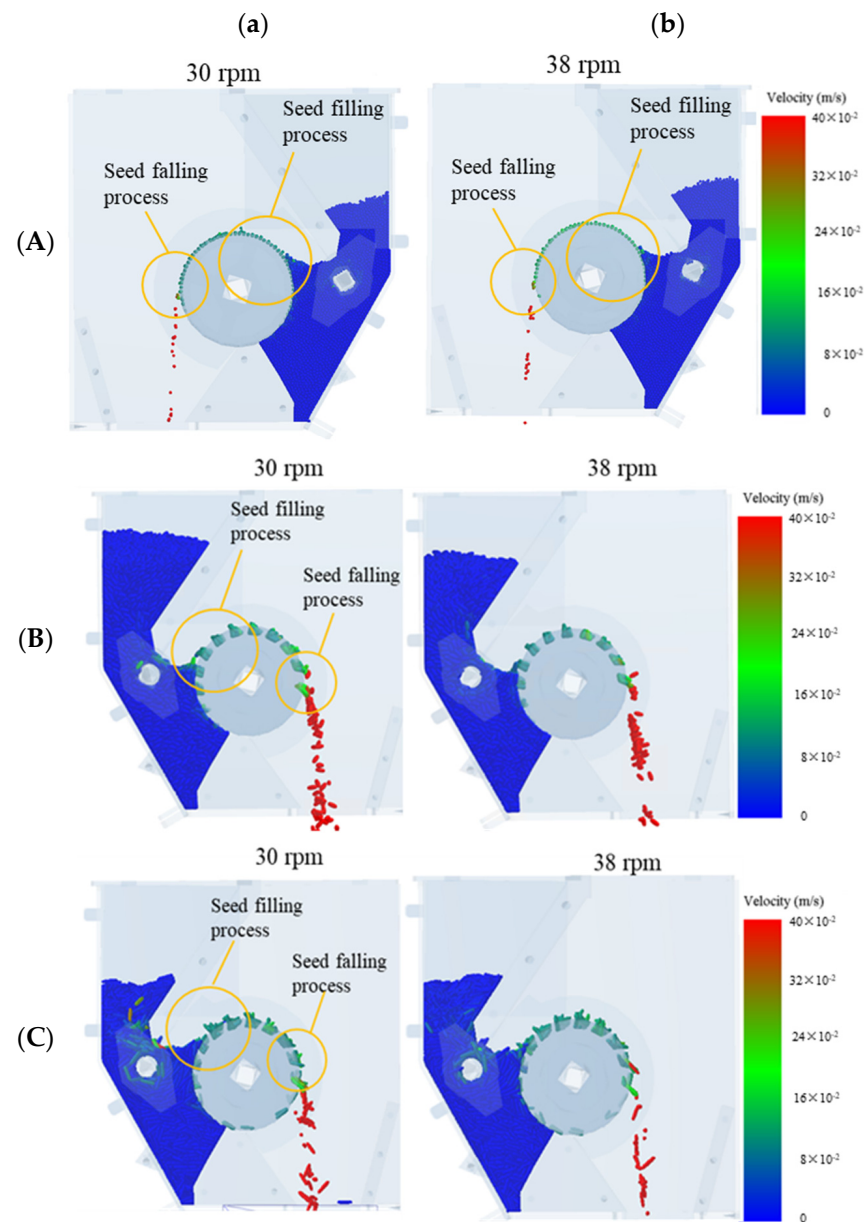
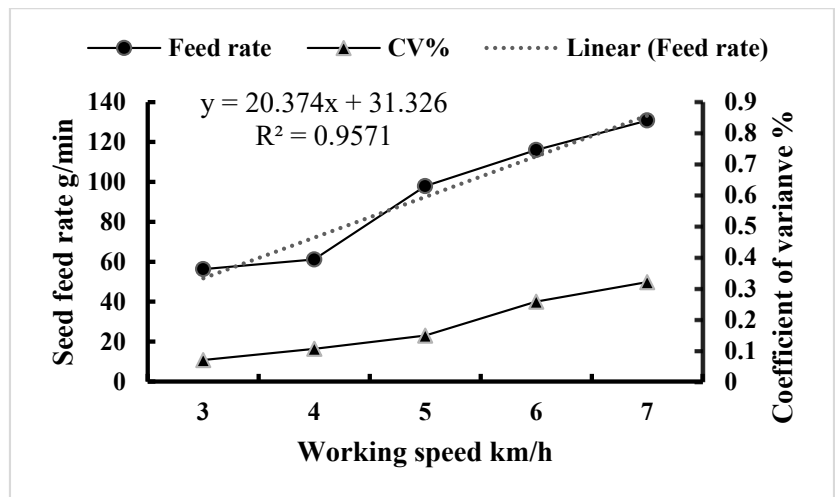


Figure 9. DEM simulation model stability test result for RWR supply at a different rotational speed. (A) Simulation test result of rapeseed supply at different rotational speeds. (B) Simulation test result of wheat supply at different rotational speeds. (C) Simulation test result of rice supply at different rotational speeds. (a) Seed supply at rotational speed 30 r/min. (b) Seed supply at rotational speed 38 r/min.

4.2. Static Workbench Experiments

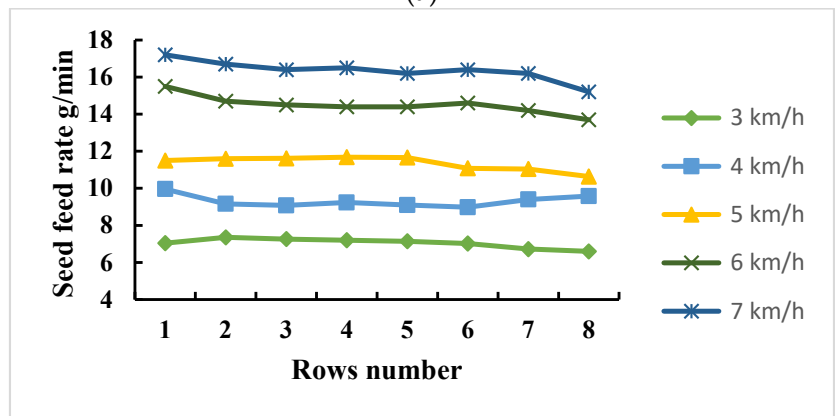
4.2.1. Effect of Working Speed of Type Hole Wheel on Feeding Rate

To explore the influence of hole wheel rotation working speed on seed supply performance, a single-factor test was conducted to determine the optimal working speed range for RWR. The test speed range was set at 3–7 km/h, with increments of 1 km/h, and each level was repeated five times to calculate the average value. The test results are shown in Figure 10A–C. The results indicated that the seed supply rate increased linearly, while the CV of seed supply stability increased slowly at lower speeds and more rapidly at higher speeds. However, this improvement in the feeding rate was accompanied by an increase in the CV.

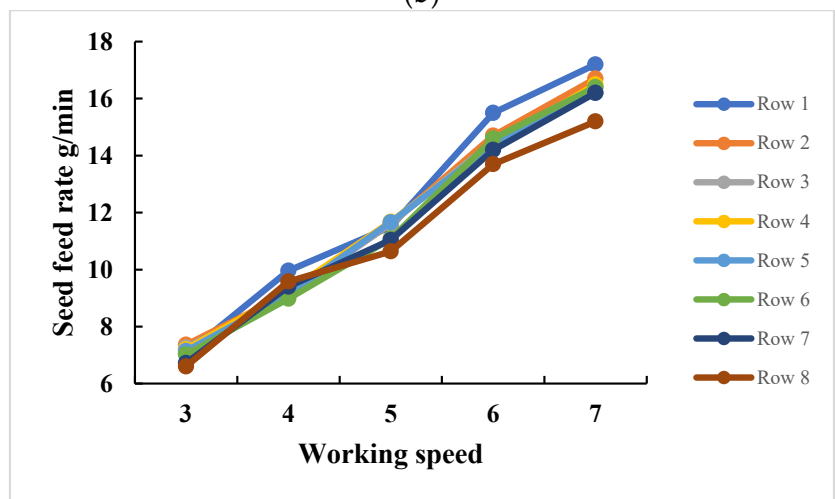


(a)

(A)

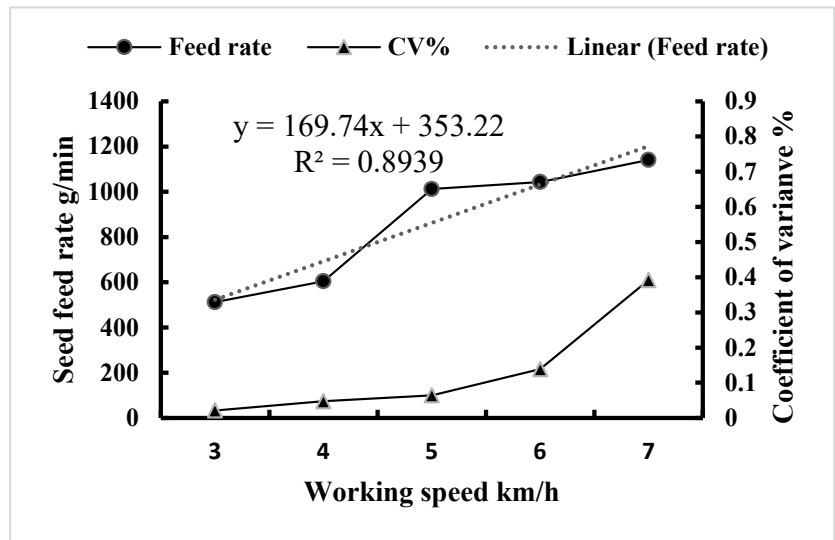


(b)



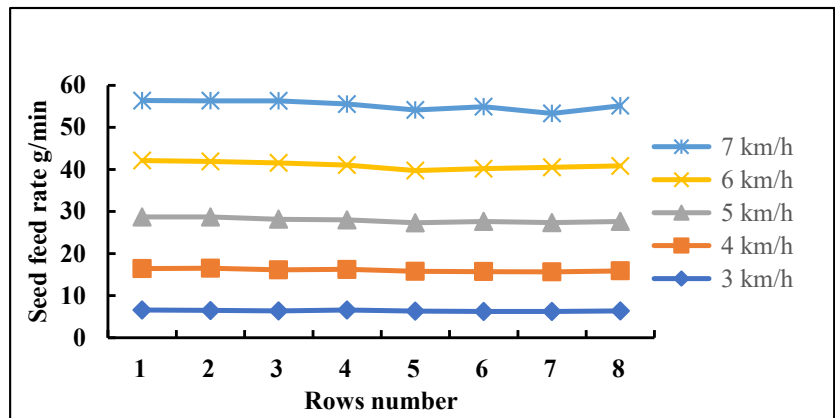
(c)

Figure 10. Cont.

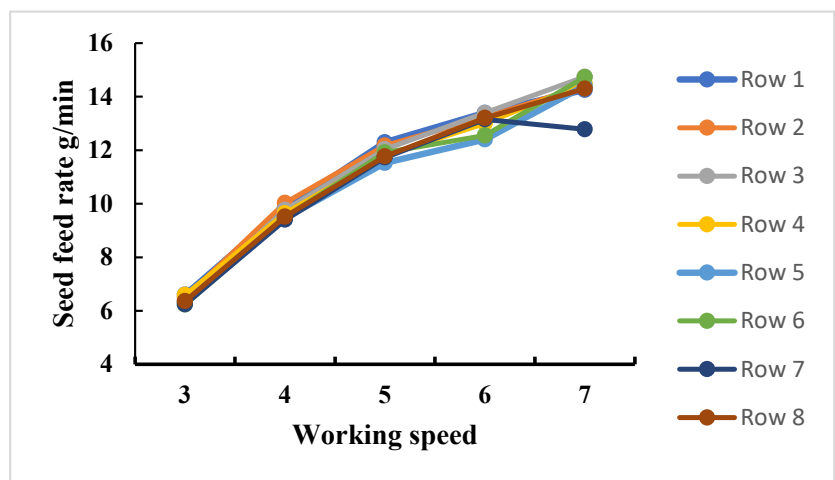


(a)

(B)

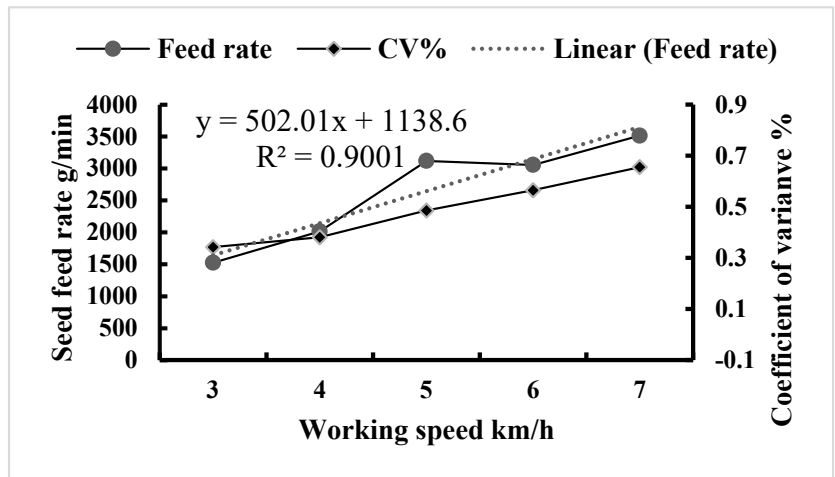


(b)

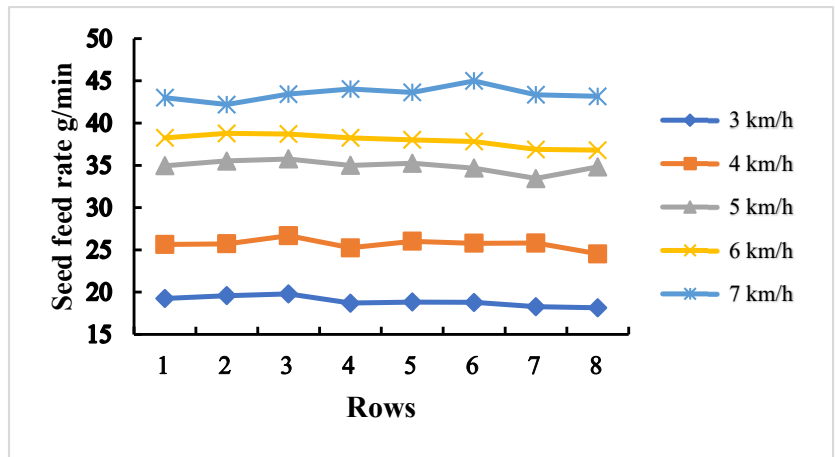


(c)

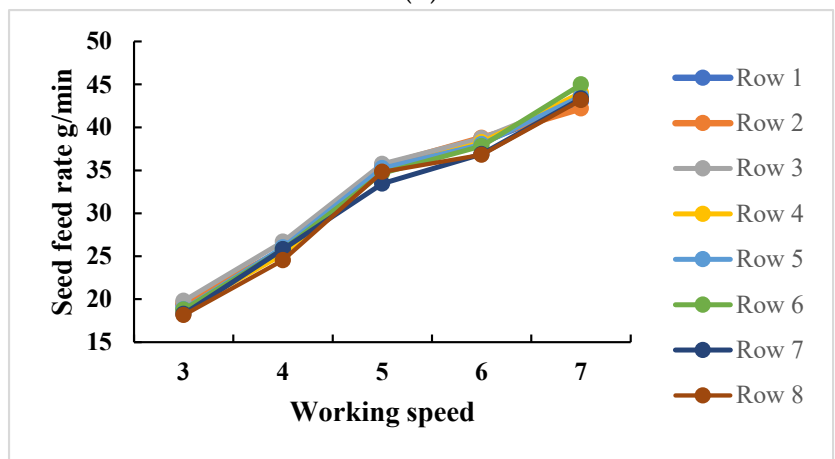
Figure 10. Cont.



(a)



(b)



(c)

Figure 10. Seeding performance of CADSD for RWR. **(A)** Rapeseed seeding performance. **(B)** Rice seeding performance. **(C)** Wheat seeding performance. (a) Total seed feed rates and coefficient of variation with respect to the working speed of the hole wheel; (b) Comparison of seed feed rates of each row; (c) Variations of seeding feed rates of each row with respect to the working speed of the hole wheel.

It can be seen from Figure 10 that across all seed types, the seed feed rate increased with an increase in the rotational working speed of the hole wheel (from 3 to 7 km/h), the same as Li Xiaoran et al. [26] and Huang et al. [32] found. Additionally, the CV of the seeding rate between each row was low, with maximum values of 0.068% and 0.32% for rapeseed, 0.342% and 0.654% for wheat, and 0.02118% and 0.391% for rice. This indicates that the system ensures uniformity and stability in both the total seeding feed rate and the seeding feed rate of individual rows. Furthermore, the optimal operating speed for seed feeding lies between 4 and 5 km/h, where seed-feeding rates for rice and wheat remain high, and CV values are low, indicating better uniformity and stability than at higher speeds. Moreover, the total seeding feed rate Y (g/min) increased with the working speed of the hole wheel X (km/h) according to a polynomial fitting for rapeseed $Y = 20.374x + 31.326$ with $R^2 = 0.9571$, rice $Y = 169.74x + 353.22$ with $R^2 = 0.8939$, and wheat $Y = 502.01x + 1138.6$ $R^2 = 0.9001$.

4.2.2. Analysis of Interaction Effects Between Rotating Speed and Seed Density

The findings presented in Table 4 indicate a linear relationship between the weight of seeds sowed and the growth in X . This discovery is logically consistent, as supported by studies that focus on a single element and the examination of how increasing the speed of the hole wheel rotation affects the seeding rate, which is found to be higher. The weight of the seeds increases proportionally with the product of the density and volume.

Table 4. Average data from the conducted experiments.

Independent Variables		Dependent Variables
X (km/h)	Y (kg/m ³)	Z (g)
3	1060	46.34
3	1125	411.9
3	1350	1523.47
4	1060	61.18
4	1125	604.06
4	1350	2014.66
5	1060	0097.92
5	1125	1012.08
5	1350	3116.62

Note: X = working speed of the seed drill hole wheel, km/h, Y = density of the seeds, kg·m³, Z = Sowed seed quantity, g.

The factors analysis in Table 5 shows that X has a more substantial impact on the change in Z compared to Y , also found by [5]. X accounts for about 94.21% of this change, while Y contributes around 5.66%. To summarize, the combined influence of both components explains approximately 99.87% of the variation in Z . The current analysis attributes only 0.13% of this difference to factors that were not disclosed. According to these results, it is necessary to fulfill this condition to do a regression analysis using only the two factors, Y and X , as presented in Table 6.

Table 5. Factor analysis, Eigenvalues (Y ; X), extraction: principal components.

Variable	Eigenvalue	Total, %	Cumulative, Eigenvalue	Cumulative, %
X	2.428×10^8	94.21	2.428×10^8	94.21
Y	2.566×10^4	5.66	2.566×10^4	99.87

Table 6. Results of regression analysis.

Variable	Beta	Std. Err.	t (4)	p-Level
X	−1.711	0.554	−3.086	0.037
Y	1.670	0.152	11.009	0.0004
X ²	1.797	0.521	3.445	0.026
X × Y	−1.288	0.247	−5.214	0.006

The resulting regression model is described as follows:

$$Z = -8 X + 0.616 Y + 0.126 X^2 - 0.010 XY \tag{13}$$

The revised multiple correlation coefficient, $R^2 = 0.937$, signifies a substantial association between the selected parameters and the observed variable. As shown in Figure 11, this indicates that X and Y significantly impact Z, accounting for approximately 99.87% of the observed variation. From this information, we may deduce that the regression model obtained from the completed experiments is extremely reliable, with a significance level of $p < 0.0029$. According to the authors of [5], this condition is necessary for predicting and resolving optimization challenges.

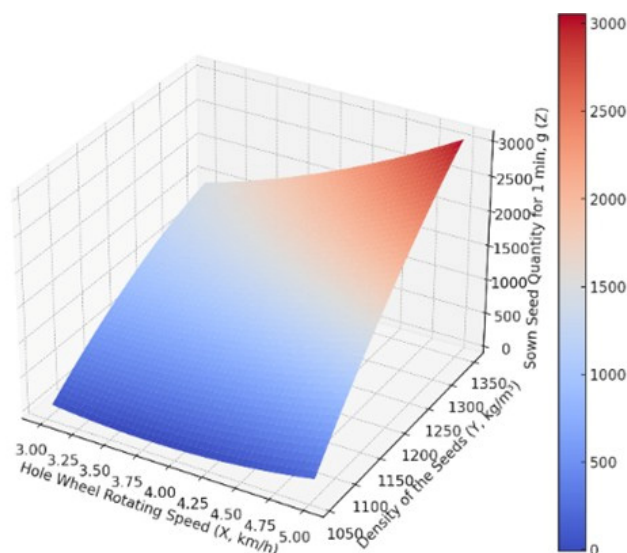


Figure 11. Regression surface for the correlation $Z = f(X, Y)$ between the quantity planted, seed density, and hole wheel rotation speed.

4.2.3. Regression Model Validation Test Results

The test results are presented in Table 7. Based on these results, we can see that the relative error between the test’s actual feed rate value and the theoretical rate value of the seed supply rate of RWR is around 2%.

Table 7. Regression model validation test result.

Crop	RS (r/min)	TR (g/min)	AR (g/min)	CV%	RE%
Wheat	30	2000	2014.66	0.31	0.73
	38	3100	3116.62	0.53	0.53
Rice	30	600	604.060	0.06	0.67
	38	1000	1012.08	0.09	1.2
Rapeseed	30	60	61.18	0.15	1.96
	38	100	97.92	0.10	2.08

Notes: RS = Rotational speed; TR = Theoretical feed rate; AR = Actual feed rate; RE = Relative error.

The empirical data show a strong correspondence with theoretical expectations, with wheat displaying relative errors of only 0.73% and 0.53%, rice with errors of 0.67% and 1.2%, and rapeseed at 1.96% and 2.08%, respectively. These results demonstrate the precise delivery of seeds in the system, highlighting its strong performance and efficient seed dispersal, providing a solid basis for controlling the seed rate of seeds sown in the CADSD.

4.3. Field Experiment Results and Discussion

The comprehensive performance testing of the seeder shown in Figure 12 involved taking the average value from five repeated measurements for each indicator. The specific test data are shown in Table 8. During field operations, multiple tasks, such as treading and fertilizing, are performed simultaneously, increasing the seeder’s resistance and generating stronger vibrations. Consequently, the qualification index for the field test is lower than that for the seeding performance test.

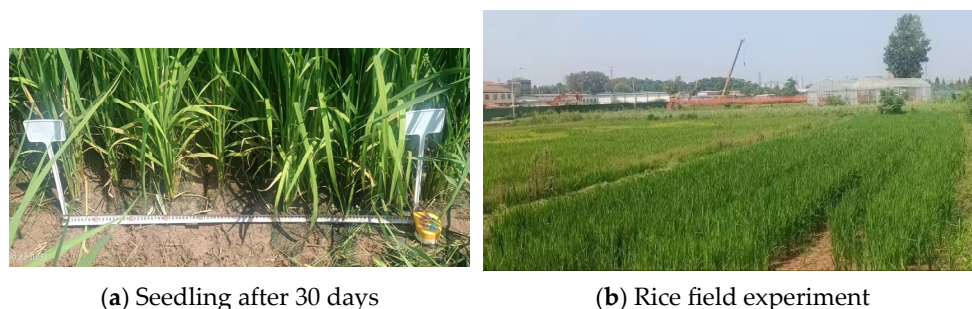


Figure 12. Rice field experiment.

Table 8. Prototype field test results.

Parameter	Qualification Index	Test Value
Seeding uniformity coefficient of variation CV%	3.89	3.44
Emergence rate %	89	88
The number of seedlings	27	26.5

It can be seen from Table 8 that the CV achieved 3.44, which is lower than the qualification index of 3.89, indicating that the seeder maintained good stability and accuracy in placing seeds uniformly across the rows. Additionally, the emergence rate during the field test was 88%, just below the qualification index of 89%. Furthermore, the number of seedlings recorded was 26.5, slightly lower than the qualification index of 27. This minor difference in emergence rate, %, uniformity coefficient of variation, CV, and the number of seedlings due to field variability, environmental conditions, and minor mechanical fluctuations caused by fieldwork vibrations indicate that, even under the challenging conditions of fieldwork, the seeder maintained a nearly optimal qualification index.

In considering the results, it is important to acknowledge that the study focused on controlled testing environments to measure the performance metrics of the sowing system precisely. This approach was chosen to ensure accurate evaluation by minimizing external variables. While field tests are essential for real-world validation, the initial phase prioritized establishing a robust understanding of the system’s capabilities. More extensive field trials are planned for future research to validate the system under diverse environmental conditions.

5. Conclusions

This study was conducted to investigate the performance of a CADSD for RWR using several tests. Research results were concluded as follows:

1. The CADSD, with the new modifications, reduces operational complexity and costs and increases agricultural seeding efficiency;
2. The bench single-factor test findings prove that the seed feed rate increases as the rotational speed rises from 3 to 7 km/h. low CV between rows indicates that the seeder maintains precision and stability across different crops;
3. A regression model verification test revealed that the relative error between the theoretical and actual test values for RWR was less than 2%;
4. A study examining the impact of seed density and rotating speed on feeding rate, factorial analysis, and regression modeling revealed that rotating speed has a significantly greater influence on the feeding rate than other factors;
5. Field experiments were conducted during the rice sowing season to validate the CADSD sowing system. The seeding uniformity was measured at a coefficient of variation CV of 3.44%, and the crop emergence rate was 88%;
6. It is strongly recommended that further modifications are required to manage increased resistance and vibrations during simultaneous fieldwork.

Author Contributions: Conceptualization, A.H.A.; methodology, L.W.; software, A.H.A.; validation, J.L. and L.W.; formal analysis, A.H.A.; investigation, A.D.A. and L.W.; resources, Q.L.; data curation, A.H.A.; writing—original draft preparation, A.H.A.; writing—review and editing, L.W. and Q.L.; visualization, J.L.; supervision, Q.L.; project administration, Q.L.; funding acquisition, Q.L. All authors have read and agreed to the published version of the manuscript.

Funding: This research was financially supported by the China Agriculture Research System of MOF and MARA (CARS-12).

Institutional Review Board Statement: Not applicable.

Informed Consent Statement: Informed consent was obtained from all subjects involved in the study.

Data Availability Statement: The data presented in this study are available on request from the corresponding author.

Conflicts of Interest: The authors declare no conflicts of interest.

References

1. Zhang, M.; Wang, Z.; Luo, X.; Zang, Y.; Yang, W.; Xing, H.; Wang, B.; Dai, Y. Review of precision rice hill-drop drilling technology and machine for paddy. *Int. J. Agric. Biol. Eng.* **2018**, *11*, 1–11. [[CrossRef](#)]
2. Wang, C.; Li, H.; Wang, J.; He, J.; Wang, Q.; Lu, C. CFD Simulation and Optimization of a Pneumatic Wheat Seeding Device. *IEEE Access* **2020**, *8*, 214007–214018. [[CrossRef](#)]
3. Alizadeh, M.; Allameh, A. Soil properties and crop yield under different tillage methods for rapeseed cultivation in paddy fields. *J. Agric. Sci.* **2015**, *60*, 11–22. [[CrossRef](#)]
4. Jin, Z.; Mu, Y.; Li, Y.; Nie, L. Effect of different rice planting methods on the water, energy, and carbon footprints of subsequent wheat. *Front. Sustain. Food Syst.* **2023**, *7*, 1173916. [[CrossRef](#)]
5. Kehayov, D.; Atanasov, A.; Bozhkov, I.; Zahariev, I. Influence of seed density and gear ratio on quantity of sowed seeds. In Proceedings of the 21st International Scientific Conference Engineering for Rural Development, Latvia University of Life Sciences and Technologies, Jelgava, Latvia, 25–27 May 2022; pp. 194–198.
6. Shah, K.; Alam, M.S.; Nasir, F.E.; Qadir, M.U.; Haq, I.U.; Khan, M.T. Design and Performance Evaluation of a Novel Variable Rate Multi-Crop Seed Metering Unit for Precision Agriculture. *IEEE Access* **2022**, *10*, 133152–133163. [[CrossRef](#)]
7. Xue, P.; Xia, X.; Gao, P.; Ren, D.; Hao, Y.; Zheng, Z.; Zhang, J.; Zhu, R.; Hu, B.; Huang, Y.; et al. Double-Setting Seed-Metering Device for Precision Planting of Soybean at High Speeds. *Trans. ASABE* **2019**, *62*, 187–196. [[CrossRef](#)]
8. Ahmad, F.; Adeel, M.; Qiu, B.; Ma, J.; Shoaib, M.; Shakoor, A.; Chandio, F.A. Sowing uniformity of bed-type pneumatic maize planter at various seedbed preparation levels and machine travel speeds. *Int. J. Agric. Biol. Eng.* **2021**, *14*, 165–171. [[CrossRef](#)]
9. Hai, N.T.; Chosa, T.; Tojo, S.; Thi-Hien, N. Application of a similarity measure using fuzzy sets to select the optimal plan for an air-assisted rice seeder. *Appl. Sci.* **2021**, *11*, 6715. [[CrossRef](#)]
10. Abdallah, A.D.; Liao, Q.; Ibrahim, E.J.; Wang, L. Design and experiment of the pneumatic cylinder type precision metering system for wheat. *Int. J. Agric. Biol. Eng.* **2023**, *16*, 88–94. [[CrossRef](#)]
11. Dengyu, X.; Wu, M.; Xie, W.; Liu, R.; Luo, H. Design and experimental study of the general mechanical pneumatic combined seed metering device. *Appl. Sci.* **2021**, *11*, 7223. [[CrossRef](#)]
12. Gao, X.; Xie, G.; Li, J.; Shi, G.; Lai, Q.; Huang, Y. Design and validation of a centrifugal variable-diameter pneumatic high-speed precision seed-metering device for maize. *Biosyst. Eng.* **2023**, *227*, 161–181. [[CrossRef](#)]

13. Jin, M.; Ding, Y.; Yu, H.; Liu, H.; Jiang, Y.; Fu, X. Optimal structure design and performance tests of seed metering device with fluted rollers for precision wheat seeding machine. *IFAC-PapersOnLine* **2018**, *51*, 509–514.
14. Li, Q.; Feng, J.; Jiang, W. Design and experiment on precision seed metering device for narrow-row and dense planting of soybean. *INMATEH Agric. Eng.* **2022**, *67*, 353–363. [[CrossRef](#)]
15. Wang, J.; Tang, H.; Wang, J.; Li, X.; Huang, H. Optimization design and experiment on ripple surface type pickup finger of precision maize seed metering device. *Int. J. Agric. Biol. Eng.* **2017**, *10*, 61–71.
16. Twizerimana, A.; Niyigaba, E.; Mugenzi, I.; Ngnadong, W.A.; Li, C.; Hao, T.Q.; Shio, B.J.; Hai, J.B. The Combined Effect of Different Sowing Methods and Seed Rates on the Quality Features and Yield of Winter Wheat. *Agriculture* **2020**, *10*, 153. [[CrossRef](#)]
17. Grossnickle, S.C.; Ivetić, V. Direct Seeding in Reforestation—A Field Performance Review. *Reforesta* **2017**, *4*, 94–142. [[CrossRef](#)]
18. Yatskul, A.; Lemiere, J.-P. ScienceDirect Influence of the divider head functioning conditions and geometry on the seed's distribution accuracy of the air-seeder. *Biosyst. Eng.* **2017**, *161*, 120–134. [[CrossRef](#)]
19. Kumar, V.J.F.; Durairaj, C.D. Influence of head geometry on the distributive performance of air-assisted seed drills. *J. Agric. Eng. Res.* **2000**, *75*, 81–95. [[CrossRef](#)]
20. Mudarisov, S.; Badretdinov, I.; Rakhimov, Z.; Lukmanov, R.; Nurullin, E. Numerical simulation of two-phase “Air-Seed” flow in the distribution system of the grain seeder. *Comput. Electron. Agric.* **2020**, *168*, 105151. [[CrossRef](#)]
21. Zhang, X.H.; Wang, Y.Z.; Zhang, L.; Peng, C.J.; Fan, G.J. Design and experiment of wheat pneumatic centralized seeding distributing system. *Nongye Jixie Xuebao/Trans. Chin. Soc. Agric. Mach.* **2018**, *49*, 59–67.
22. Yang, S.; Liao, Y.; Liao, Q. Experimental study on pneumatic seed-metering system of 2BFQ-6 precision planter for rapeseed. *Trans. Chin. Soc. Agric. Eng.* **2012**, *18*, 57–62.
23. Akhalaya, B.K.; Gromov, V.V.; Gaiko, O.A.; Akopyan, A.S. New metering device for pneumatic seeding machine. In Proceedings of the Innovative Technologies in Science and Education (ITSE 2020 Conference), Divnomorskoe Village, Russia, 19–30 August 2020; pp. 472–474.
24. Tarasenko, V.; Bondarenko, L.; Shcherbakova, N.; Horbova, N. Sowing Units for Drilling Vegetable Crops. In *Modern Development Paths of Agricultural Production*; Nadykto, V., Ed.; Springer: Berlin/Heidelberg, Germany, 2019; pp. 289–298.
25. Baoshan, W.; Lei, W.; Yitao, L.; Chong, W.U.; Mei, C.A.; Qingxi, L. Design and test of seeding wheels of precision hole-seeding centralized metering device for small particle size seeds. *Nongye Jixie Xuebao/Trans. Chin. Soc. Agric. Mach.* **2022**, *53*, 64–76.
26. Li, X.; Liao, Q.; Wang, L.; Li, M.; Du, W. Design and experiments of the type-hole wheel with high-speed air-assisted centralized metering device for rice, wheat and rapeseed. *Nongye Gongcheng Xuebao/Trans. Chin. Soc. Agric. Eng.* **2023**, *39*, 35–48.
27. Vaishnavi, D.; Rathinakumari, A.C.; Kumaran, G.S. Physical and Engineering Properties of Vegetable Seeds Relevant for Development of Protray Vacuum Seeder for Vegetable Nursery. *Andhra Agric. J.* **2018**, *65*, 179–183.
28. Li, Z.; Zhong, J.; Gu, X.; Zhang, H.; Chen, Y.; Wang, W.; Zhang, T.; Chen, L. DEM Study of Seed Motion Model-Hole-Wheel Variable Seed Metering Device for Wheat. *Agriculture* **2023**, *13*, 23. [[CrossRef](#)]
29. Lei, X.L.; Yang, W.H.; Yang, L.J.; Liu, L.Y.; Liao, Q.X.; Ren, W.J. Design and experiment of seed hill feeding device in pneumatic centralized metering device for hybrid rice. *Trans. CSAM* **2018**, *49*, 58–67.
30. GB/T 25418-2022; Method of Grain Direct Seeding Machine. China Agriculture Press: Beijing, China, 2022.
31. Wu, Z.; Li, M.; Lei, X.; Wu, Z.; Jiang, C.; Zhou, L.; Ma, R.; Chen, Y. Simulation and parameter optimisation of a centrifugal rice seeding spreader for a UAV. *Biosyst. Eng.* **2020**, *192*, 275–293. [[CrossRef](#)]
32. Huang, X.; Zhang, S.; Luo, C.; Li, W.; Liao, Y. Design and Experimentation of an Aerial Seeding System for Rapeseed Based on an Air-Assisted Centralized Metering Device and a Multi-Rotor Crop Protection UAV. *Appl. Sci.* **2020**, *10*, 8854. [[CrossRef](#)]

Disclaimer/Publisher’s Note: The statements, opinions and data contained in all publications are solely those of the individual author(s) and contributor(s) and not of MDPI and/or the editor(s). MDPI and/or the editor(s) disclaim responsibility for any injury to people or property resulting from any ideas, methods, instructions or products referred to in the content.